Applied Catalysis B: Environmental 99 (2010) 222–228

Contents lists available at ScienceDirect

Applied Catalysis B: Environmental

journal homepage: www.elsevier.com/locate/apcatb

Microfibrous-structured silver catalyst for low-temperature gas-phase selective oxidation of benzyl alcohol

Miaomiao Deng, Guofeng Zhao, Qingsong Xue, Li Chen, Yong Lu*

Shanghai Key Laboratory of Green Chemistry and Chemical Processes, Department of Chemistry, East China Normal University, Shanghai 200062, China

ARTICLE INFO

Article history:
Received 1 December 2009
Received in revised form 12 June 2010
Accepted 15 June 2010
Available online 19 June 2010

Keywords:
Silver catalysis
Micro-structured packings
Nickel fiber
Benzyl alcohol
Selective oxidation

ABSTRACT

A highly active and selective silver on nickel fiber catalyst was successfully prepared for selective oxidation of benzyl alcohol. The Ag/Ni catalyst was obtained by loading Ag (10 wt%) on paper-like microfibrous structure (consisting of 5 vol% of 8-μm Ni-fiber) by impregnation method. The wettability of Ni-fiber support was vastly improved by a simple water pre-wetting and overnight drying treatment process. This yielded a catalyst (Ag/Ni-fiber-M) with more Ag cations and selectively active oxygen species than the catalyst (Ag/Ni-fiber) using the untreated support. The Ag/Ni-fiber-M showed much higher low-temperature activity/selectivity than the Ag/Ni-fiber, which could be attributed to the differences in their silver morphology and particle size. The best conversion and benzaldehyde selectivity observed were both 97% for Ag/Ni-fiber-M at 300 °C, and 91 and 84% for Ag/Ni-fiber at 380 °C, respectively. Benzyl alcohol selective oxidation would proceed concurrently through both direct O_2 activation route and NiO_x-participating oxygen spillover route. Formation of Ni_xC phase occurred and hampered the latter reaction route thereby leading to partial deactivation. However, spent catalyst could restore activity through an oxidation treatment at 400 °C.

1. Introduction

Carbonyl compounds such as aldehydes and ketones are very important chemicals in industrial organic synthesis [1–3]. Most of them are traditionally synthesized via the oxidation of alcohols in the presence of large amount of volatile organic solvents using stoichiometric inorganic oxidants, notably Cr reagents [1,4–6]. From a standpoint of green chemistry, however, there is an exigent demand for efficient, cost-effective and environmentally benign reaction systems that adopt a recyclable catalyst and clean oxidants such as O_2 [1,7–16].

Benzaldehyde is one of the most important compounds used in the cosmetics and flavor industries, with large consumption just after vanillin [16]. Benzylaldehyde is not only commercially produced by the hydrolysis of benzalchloride, but also can be partially obtained as a by-product from the benzoic acid industry [16,17]. In addition to the presence of organic chlorine or benzoic acid impurity that poses major concerns for the cosmetic and flavor industries, the present route does not conform to the guiding principles of green chemistry, which aims at eliminating waste, maximizing atom utilization efficiency, avoiding use of auxiliary substances including solvents, and adopting catalysts [18].

The gas-phase selective oxidation of benzyl alcohol using O_2 in the presence of heterogeneous catalyst is an attractive alternative for producing organic chlorine-/acid-free benzaldehyde [9–12,16]. The development of high-performance catalysts with a unique combination of excellent low-temperature activity/selectivity and high thermal conductivity remains challenging. Some silver-based catalysts including electrolytic silver and supported silver catalysts have been demonstrated for gas phase selective oxidation of benzyl alcohol in a packed bed reactor [9–15]. The electrolytic silver catalyst has good thermal conductivity, but is not active at temperatures below 500 °C or not highly selective at above 500 °C due to cracking and over oxidation [9,12]. Supported silver catalysts such as those using Al_2O_3, SiO_2 and SiC as supports have demonstrated better catalytic activity at relatively low temperatures [10,11]. Nevertheless, their weak thermal conductivity would induce hotspots in the reaction bed, because the great quantity of reaction heat that liberates rapidly cannot be dissipated. This is not only a main cause of catalyst degradation, but also a hidden danger such as bed temperature runaway. Recently, the Au/SiO_2 catalysts with or without copper additives have been reported to exhibit good low-temperature activity with very high target product selectivity in the gas-phase selective oxidation of benzyl alcohol [16]. However, significant bed-temperature increases of >40 °C were observed even in lab-scale experiments [16], which were attributed to their weak thermal conductivity. Hence, practical applications of these catalysts are very limited.

* Corresponding author. Tel.: +86 21 62233424; fax: +86 21 62233424.
E-mail address: ylu@chem.ecnu.edu.cn (Y. Lu).

0926-3373/$ – see front matter © 2010 Elsevier B.V. All rights reserved.
doi:10.1016/j.apcatb.2010.06.023

As a strategy, a new class of silver catalysts supported on sinter-locked 8-μm Ni-fibers has been developed for gas-phase selective oxidation of benzyl alcohol to benzaldehyde [12]. These microfibrous-structured silver catalysts exhibit much higher activity/selectivity and provide significant increase in the steady-state volumetric reaction rate with dramatic reduction in Ag loading, when compared to the electrolytic silver catalysts. In particular, benzyl alcohol conversion of 91% is achievable with benzaldehyde selectivity of ~85% at 380 °C, corresponding to product yield of ~77% [12]. Despite the observed high conversion and selectivity, maximization of benzaldehyde yield is particularly desirable for simplifying the subsequent purification. In this regard, sinter-locked Ni-fiber support was found to have poor wetting property making it difficult for aqueous solution of $AgNO_3$ to spread uniformly and homogeneously. We then proposed that the performance of Ag/Ni-fiber catalysts might be significantly promoted by improving the wettability of Ni-fiber support. In general, sinter-locked Ni-fibers were easily made wettable by a simple pre-wetting treatment with water and subsequently drying at 120 °C. As a result, the as produced catalysts provided a significant promotion of low-temperature activity/selectivity. In order to elucidate the factors contributing to the enhanced catalyst performance, the catalytically relevant physiochemical properties and structure–performance relationship were investigated and discussed herein. In addition, catalyst reaction/regeneration cycle tests were also carried out to gain insight into catalyst deactivation.

2. Experimental

The thin-sheet sinter-locked Ni-fiber support with three-dimensional network was fabricated by regular wet-lay papermaking/sintering processes using 8-μm diameter by 2–3 mm length Ni-fiber chops, as described in detail previously [19–22]. The resulting microfibrous support consisting of 5% (vol%) Ni-fibers with 95% (vol%) void volume was wetted by spraying with water and then dried overnight at 120 °C in air. Silver (10 wt%) was loaded onto microfibrous nickel support by the incipient wetness impregnation method using $AgNO_3$ precursor, then activated by calcination in air at 600 °C for 4 h. The as-prepared catalyst was described as Ag/Ni-fiber-M. The preparation of the previously reported Ag/Ni-fiber catalyst [12] followed the same procedures, except without the additional water wetting treatment step. Silver loading was determined by inductively coupled plasma atomic emission spectrometry (ICP-AES) on a Thermo Scientific iCAP 6300 ICP spectrometer, which indicated that the Ag contents were 9.9 and 9.7 wt% for the Ag/Ni-fiber-M catalyst and Ag/Ni-fiber catalyst, respectively.

Gas-phase selective oxidation reactions of benzyl alcohol were carried out in a quartz tubular reactor (i.d. 14 mm) heated by a temperature-controlled tube furnace under atmospheric pressure as described previously [12]. 20 g benzyl alcohol was fed into reactor bed per hour per gram of catalyst by a precious liquid pump, i.e., weight hourly space velocity (WHSV) was 20 h^{-1}. Control experiments on the Ni-fiber supports calcined in air at temperature ranged from 300 to 600 °C were performed, inducing the conversion of <17% and the target product selectivity of <60%.

Ag/Ni-fiber-M and Ag/Ni-fiber catalysts were characterized by X-ray diffraction (XRD, Bruker D8 ADVANCE diffractometer (Cu Kα)), scanning electron microscope (SEM, Hitachi S-4800) equipped with an energy dispersive X-ray analyses (EDX) unit (Oxford, UK), and UV–visible diffuse reflectance spectroscopy (UV–vis DRS, Shimadzu UV-2400PC). The catalysts were also studied by oxygen temperature programmed desorption (O_2-TPD) on a Quantachrome ChemBET 3000 chemisorption apparatus with a TCD. Carbon content on the used catalyst samples was determined using a Mettler TG-SDTA-851 analyzer.

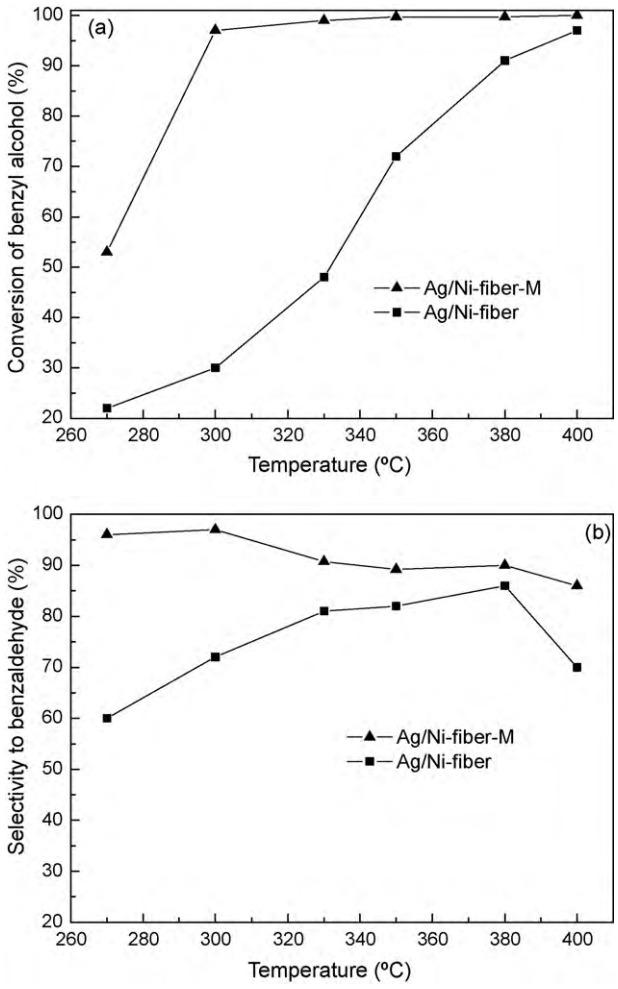

Fig. 1. Conversion (a) and target product selectivity (b) versus reaction temperature over the Ag/Ni-fiber-M and Ag/Ni-fiber catalysts for gas-phase selective oxidation of benzyl alcohol to benzaldehyde. O_2/hydroxyl = 0.6 and WHSV = 20 h^{-1}.

3. Results and discussion

3.1. Catalytic behavior

Fig. 1 shows the plots of conversion and target product selectivity versus reaction temperature using Ag/Ni-fiber-M and Ag/Ni-fiber as catalysts for the selective oxidation of benzyl alcohol using an O_2/hydroxyl molar ratio of 0.6 and WHSV of 20 h^{-1}. It is obvious that Ag/Ni-fiber-M is superior in both activity and selectivity to the Ag/Ni-fiber within the entire temperature range. In addition, their reactivity profile is quite different. For Ag/Ni-fiber-M, conversion increased sharply from 53 to 97% when the reaction temperature was increased from 270 to 300 °C and then approaches to 100% at 400 °C; benzaldehyde selectivity remained at 97% until 300 °C, but then decreased slowly at 400 °C. For Ag/Ni-fiber, conversion increased with increasing temperature, but the best selectivity of 86% was observed at 380 °C. The maximum benzaldehyde yield of ~95% was obtained using Ag/Ni-fiber-M at 300 °C, which is much higher than that of only ~76% with Ag/Ni-fiber at 380 °C. In addition, a significant difference in benzaldehyde selectivity was observed between Ag/Ni-fiber-M and Ag/Ni-fiber (97 vs. 60%) at 270 °C and the main by-product was benzoic acid for Ag/Ni-fiber. Weakly adsorbed oxygen is likely formed with Ag/Ni-fiber catalyst,

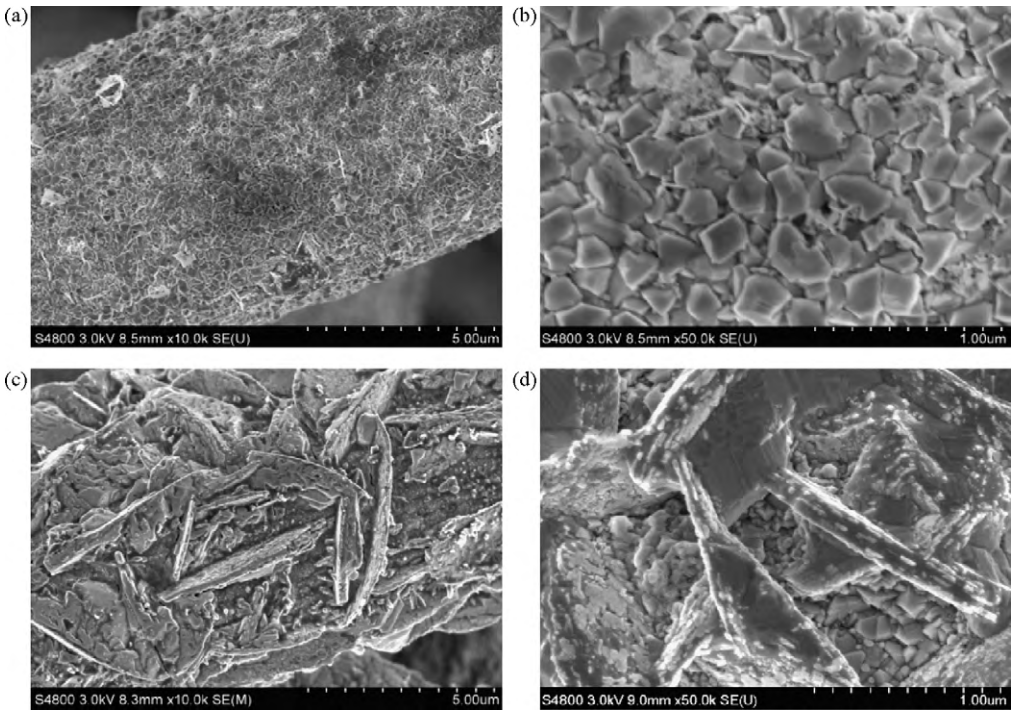

Fig. 2. SEM images of the Ag/Ni-fiber (a,b) and Ag/Ni-fiber-M (c,d) catalysts.

which is known to favor overoxidation of benzyl alcohol to form benzoic acid [23]. Nevertheless, most benzoic acid can remain at low temperature (e.g., byproduct selectivity at 270 °C: 27% benzoic acid; 6% benzene; 5% toluene; 2% CO_2) but decompose into benzene, toluene and CO_2 when the reaction temperature is increased (e.g., product selectivity at 400 °C: 66% benzaldehyde; 1% benzoic acid; 16% benzene; 2% toluene; 15% CO_2).

We also examined the influences of Ag loading (from 1 to 30 wt%) and the calcination temperature (from 300 to 700 °C) on the catalytic performance of the catalysts. The best low-temperature activity/selectivity was obtained from the Ag/Ni-fiber-M catalyst sample with 10 wt% Ag loading and calcined in air at 600 °C. This is also consistent with the Ni-fiber (without wetting treatment) supported silver catalysts in our previous report [12]. In particular, over the electrolytic silver catalyst the best yield of only ~42% (benzyl alcohol conversion: ~53%, benzaldehyde selectivity: ~80%) is obtained even at 500 °C using a low WHSV of 8 h^{-1} [12].

3.2. Morphology and dispersion of silver

3.2.1. SEM

Fig. 2 shows the SEM images of Ag/Ni-fiber-M and Ag/Ni-fiber catalysts, illustrating significant difference in morphology of the silver grains. For the Ag/Ni-fiber catalyst, a rimous layer making up of a number of 200–300 nm fragments with relatively regular shape is observed on the fiber surface (Fig. 2a and b). The EDX element analyses indicate that these fragments are small silver grains. Fig. 2b also indicates that the silver grains have mirror-like surfaces. For the Ag/Ni-fiber-M catalyst, an intersecting structure comprised of slice-like silver grains (conformed by EDX analyses) was formed, which is abundant in grain boundaries (Fig. 2c and d). In addition, abundant terrace substructures (~10 nm thick by ~100 nm width) are clearly observed on the slice-like silver grains (Fig. 2d). These features differ considerably from the mirror-like surfaces of the silver grains on the Ag/Ni-fiber catalyst.

As noted previously, surface morphology strongly affects the oxygen chemisorptive properties of the silver catalysts [23–26]. In particular, highly selective and active oxygen species that have strong silver–oxygen covalent bonds can be formed easily via both direct dissociative chemisorption of O_2 at Ag(1 1 1)-like planes on grain boundaries and surface segregation of the subsurface O along interstitial sites through grain boundaries [23–25]. It is clear that the silver morphology for Ag/Ni-fiber-M catalyst is more abundant in grain boundaries than that for Ag/Ni-fiber catalyst (Fig. 2). This feature may greatly facilitate the formation of selective and active oxygen species, leading to significant promotion of low-temperature activity/selectivity.

3.2.2. XRD

Fig. 3 shows the XRD patterns of the Ag/Ni-fiber-M and Ag/Ni-fiber catalysts. Metallic silver phase is identified by the Ag(1 1 1) peak situated at (2θ) 38.2° seen on both catalysts. It should be noticeable that the Ag(1 1 1) peak for Ag/Ni-fiber-M is broader and

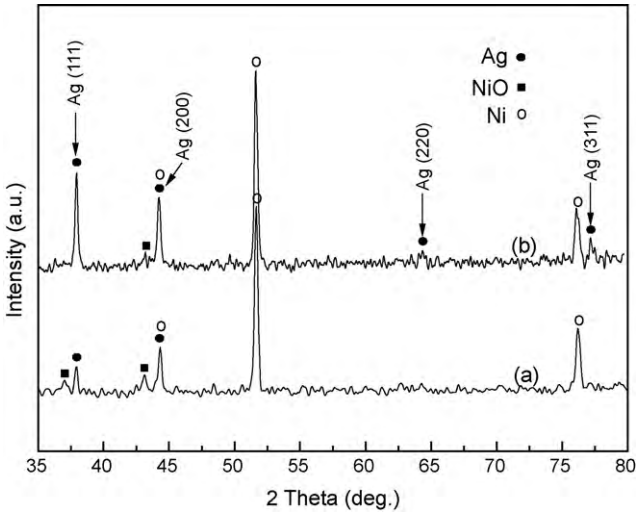

Fig. 3. XRD patterns of the Ag/Ni-fiber-M (a) and Ag/Ni-fiber (b) catalysts.

weaker than the Ag/Ni-fiber catalyst, corresponding to the estimated Ag particle sizes of ~20 nm for the former and ~40 nm for the latter. The absence of the Ag XRD patterns at (2θ) 64.4° and 77.2° on the Ag/Ni-fiber-M catalyst further confirms a better silver dispersion. Smaller metal particle size (<100 nm) can provide higher metal surface area, thereby leading to higher catalytic activity [9,27]. In addition, small amount of NiO phases are formed on both catalysts as evidenced by the weak and broad XRD peaks at 37.4° and 43.2° (Fig. 3). However, the NiO phase was found not active for oxidation of benzyl alcohol, since conversion of <17% was obtained using Ni-fiber pre-calcined in air at 600 °C under compatible reaction conditions.

Interestingly, the estimated Ag particle size of 20 nm is very close to the thickness of the terrace substructures on the Ag/Ni-fiber-M catalyst, suggesting that the slice-like silver grain is an assembly of numerous silver nano-sheets. For the Ag/Ni-fiber catalyst, however, no reasonable correlation between the estimated Ag particle size of 40 nm calculated using Scherrer's equation and the observed 100–200 nm in the SEM image (Fig. 2b) could be established.

3.3. Active sites and oxygen species

3.3.1. UV–vis DRS

Fig. 4 shows the UV–vis DRS spectra of Ag/Ni-fiber-M and Ag/Ni-fiber catalysts. According to previous UV–vis studies on the silver catalysts [9,10,28,29], three types of silver species were identified. In general, metallic silver film and big particles provide the absorption band in the region of 310–320 nm; the isolated Ag^+ ions deliver bands in the region of 230–250 nm, while charged $Ag_n^{\delta+}$ clusters correspond to bands near 270–290 nm and 370–390 nm; the band above 400 nm is attributed to metallic Ag clusters. In some cases [30], metallic Ag clusters may induce a band at 350 nm. As shown in Fig. 4a, along with a strong band at 310–320 nm, a weak band at 230–250 nm is presented as well as two faint bands at 270–290 nm and 370–390 nm. This indicates that a large amount of metallic silver particles were formed rather than isolated Ag^+ ions and charged $Ag_n^{\delta+}$ clusters on the Ag/Ni-fiber. In contrast, the band at 310–320 nm weakened dramatically while the other bands related to the Ag^+ ions and $Ag_n^{\delta+}$ clusters became strong on the Ag/Ni-fiber-M (Fig. 4b). This indicates that Ag/Ni-fiber-M has quite higher concentration of Ag^+ ions and $Ag_n^{\delta+}$ clusters than the Ag/Ni-fiber.

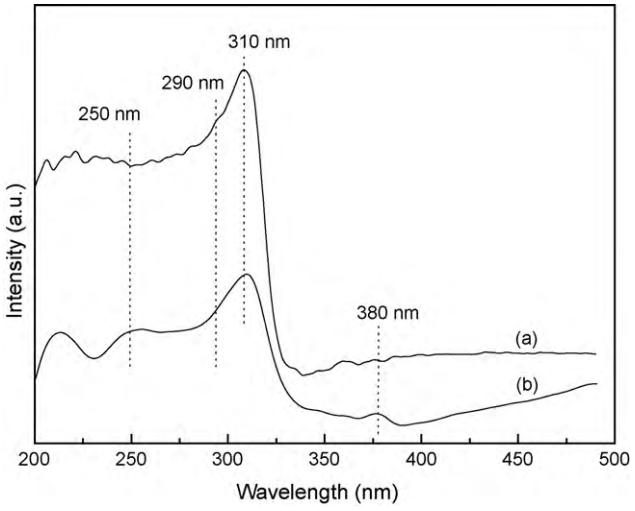

Fig. 4. UV–vis spectra of the Ag/Ni-fiber (a, Ni-fiber as background) and Ag/Ni-fiber-M (b, Ni-fiber-M as background) catalysts. *Note:* both Ni-fiber and Ni-fiber-M support offered quite similar UV spectra.

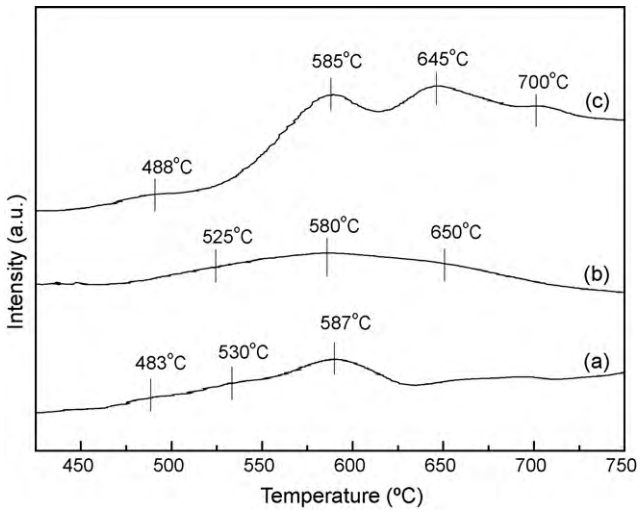

Fig. 5. O_2-TPD profiles of the Ni-fiber support (a), Ag/Ni-fiber (b), and Ag/Ni-fiber-M (c). *Note:* sample (a) was pre-calcined at 600 °C in air for 4 h.

3.3.2. O_2-TPD

Fig. 5 shows the O_2-TPD profiles for the Ag/Ni-fiber-M and Ag/Ni-fiber catalyst samples. No obviously detectable O_2 desorption proceeded below 400 °C. For reference, the O_2-TPD profile for the Ni-fiber pre-calcined at 600 °C was collected and shown in Fig. 5 (curve a). The Ni-fiber-M followed by compatible calcination offered a TPD profile quite similar to that of Fig. 5a (not shown). Series of weak peaks present at 483, 530 and 587 °C on the pre-oxidized Ni-fiber support were assigned for the O_2 desorption of surface NiO_x (Fig. 5a). Three broad and weak peaks are observed at 525, 580 and 650 °C on the Ag/Ni-fiber (Fig. 5b). The first two peaks at 525 and 580 °C are similar to the ones on the profile of the pre-oxidized Ni-fiber support (Fig. 5a) and therefore were assigned as O_2 desorption of surface NiO_x. The profile of Ag/Ni-fiber-M catalyst is comprised of four well-separated peaks at 488, 585, 645 and 700 °C. Among them, the peaks below 600 °C also could be assigned to the O_2 desorption of NiO_x on the Ni-fiber support.

Numerous studies on oxygen species on supported and unsupported silver catalysts have been performed and attributed the low-temperature desorption to weakly chemisorbed atomic oxygen (150–350 °C), the high-temperature desorption to strongly chemisorbed atomic oxygen (400–750 °C), and the desorption at above 750 °C to lattice oxygen [23,29,31–34]. Accordingly, the O_2 desorption peaks of Ag/Ni-fiber (Fig. 5b) and Ag/Ni-fiber-M (Fig. 5c), except the contributions from surface NiO_x, could all be assignable to the strongly chemisorbed oxygen on silver particles. By comparison, it is clear that the amount of strongly chemisorbed oxygen is much higher on the Ag/Ni-fiber-M catalyst than that on the Ag/Ni-fiber catalyst. In addition, the multi-peak feature of Fig. 5c is likely due to the nonuniform and complex morphology of Ag/Ni-fiber-M catalyst.

3.3.3. Discussion

The Ag^+ ions and $Ag_n^{\delta+}$ clusters have been proven active in fixing ethylene in epoxidation of ethylene [29,35,36]. Similarly, these cations are likely involved in fixing alcohol molecules in aerobic selective oxidation of alcohols. The fixed alcohols could thereby react with the selective and active oxygen neighbors on silver particles to form aldehydes. Therefore, high concentrations of these cations and the strongly chemisorbed oxygen species (responsible for selective oxidation) undoubtedly can significantly promote the selective oxidation of benzyl alcohol. Indeed, the Ag/Ni-fiber-M catalyst was found to have much more Ag cations and selectively active oxygen species than the Ag/Ni-fiber catalyst. This would explain

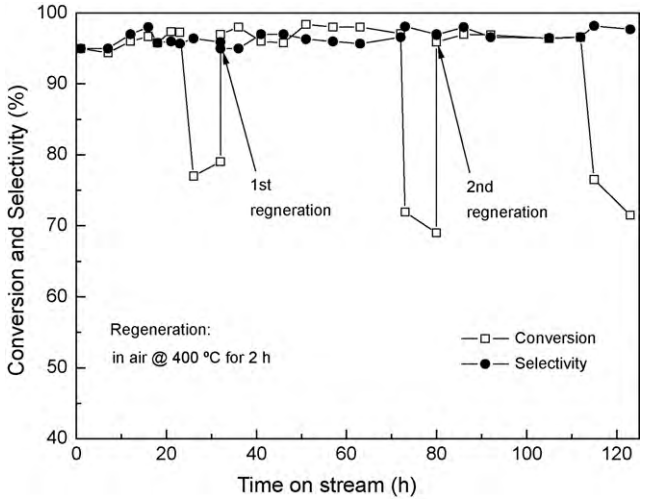

Fig. 6. Reaction/regeneration cycle tests of the Ag/Ni-fiber-M catalyst for the gas-phase selective oxidation of benzyl alcohol to benzaldehyde. Reaction temperature = 300 °C, O_2/hydroxyl = 0.6, WHSV = 20 h^{-1}; oxidative regeneration temperature = 400 °C.

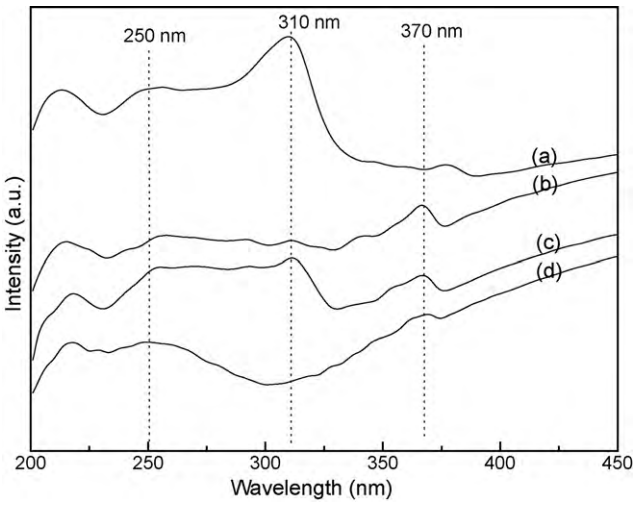

Fig. 7. UV–vis spectra of the Ag/Ni-fiber-M catalysts: (a) fresh, (b) working (after 15-h run same as in Fig. 6), (c) spent (after 23-h run same as in Fig. 6), and (d) regenerated (after 1st regeneration).

why, by nature, Ag/Ni-fiber-M catalyst provided much higher low-temperature activity for the selective oxidation of benzyl alcohol than Ag/Ni-fiber catalyst (Fig. 1). In fact, this is also in agreement with previous reports which concluded that co-existence of large amount of Ag^+ ions/$Ag_n^{\delta+}$ clusters and strongly chemisorbed atomic oxygen species can significantly promote the catalyst activity/selectivity in preferential oxidation of CO [34], formaldehyde synthesis [28] and ethylene epoxidation [29].

3.4. Deactivation and regeneration of Ag/Ni-fiber-M

3.4.1. Longer-term test

Fig. 6 shows the conversion/selectivity results of Ag/Ni-fiber-M over two regeneration cycles. Benzyl alcohol conversion remained at 94–97% within the first 23 h and then declines sharply to 70–77%. The regeneration of spent catalyst was carried out by stopping the alcohol feed, then heating the catalyst bed to 400 °C for 2 h under a flow of O_2/N_2 (11.5/100) at 111.5 mL/min. The catalytic bed temperature was reduced to 300 °C, while the alcohol feeding was restarted for the next reaction cycle. The regenerated catalyst performed similarly to fresh catalyst and delivered a conversion of >95% and target product selectivity of >97%. This indicates that the spent catalyst was able to recover its activity after a simple oxidation treatment. In addition, no deterioration in activity/selectivity of the regenerated Ag/Ni-fiber-M catalyst was observed after two reaction–regeneration cycles. Moreover, extended experiments at lower regeneration temperatures (300 and 350 °C) have not yielded the reactivity better than that regenerated at 400 °C.

It should be noted that the spent catalyst still preserves ~75% of the original activity with unchanged benzaldehyde selectivity until to start next regeneration/reaction cycle, indicating that the Ag/Ni-fiber-M catalyst showed a feature of partial deactivation. Carbon content on the catalyst samples after 2, 7, 15 and 23 h was determined by thermal gravimetric analysis (TGA) to be 0.3, 0.77, 0.84 and 0.86 wt%, respectively. This trend is in no agreement with the reaction behavior during the first 23 h as shown in Fig. 6, thus ruling out carbon covering the Ag particles for catalyst partial deactivation. It is reasonable to infer from the above results that benzyl alcohol selective oxidation would proceed likely through two parallel routes while one route seemed very easy to be hampered along with time-on-stream.

3.4.2. UV–vis, O_2-TPD and XRD characterizations

Determining the main cause for the partial deactivation will undoubtedly aid catalyst design and lead to further improvement. We first investigated whether the amount of Ag^+ ions and $Ag_n^{\delta+}$ clusters were reduced by performing UV–vis analyses of the reacted and regenerated Ag/Ni-fiber-M catalysts and the results are displayed in Fig. 7. Compatible UV bands at 230–250 nm for the Ag^+ ions and 370–390 nm for the $Ag_n^{\delta+}$ clusters were observed on all catalyst samples regardless of their states. This indicates that there is no noticeable reduction of Ag^+ ions and $Ag_n^{\delta+}$ clusters on the surfaces of the spent catalyst sample. Consequently, the deactivation of 10% Ag/Ni-fiber-M catalyst was not due to the reduction of cationic silver. In addition, the UV band at 310–320 nm due to metallic silver particles weakened remarkably for the reactive, spent and regenerated samples in comparison with the fresh one. This indicates that silver species proceed to disperse on the nickel fiber rather than aggregate to form large silver metal particles during the reaction. Actually, it has been reported that thick silver film on the nickel substrate can be torn into small particles through reactive solid state dewetting mechanism when annealed in oxidative atmosphere [37,38]. However, it should be pointed out that such dispersion of metallic Ag particles did not promote the activity since no additional Ag^+ ions and $Ag_n^{\delta+}$ clusters were produced (Fig. 7).

Table 1
Amount of strongly chemisorbed oxygen by O_2-TPD for the Ag/Ni-fiber-M catalysts.[a]

Catalyst	Fresh	Working[b]	Spent[c]	Regenerated[d]
Amount of O_{ad}, μmol O_2/g_{cat}	3.4	3.0	1.9	3.8
O_{ad} retention, %	100	88	56	112

[a] Calculation of O_{ad} amount was based on the dominant O_2-TPD peak at around 650 °C.
[b] Equivalent to the sample after 15-h run in Fig. 6.
[c] Equivalent to the sample after 23-h run in Fig. 6.
[d] Equivalent to the sample after 1st regeneration.

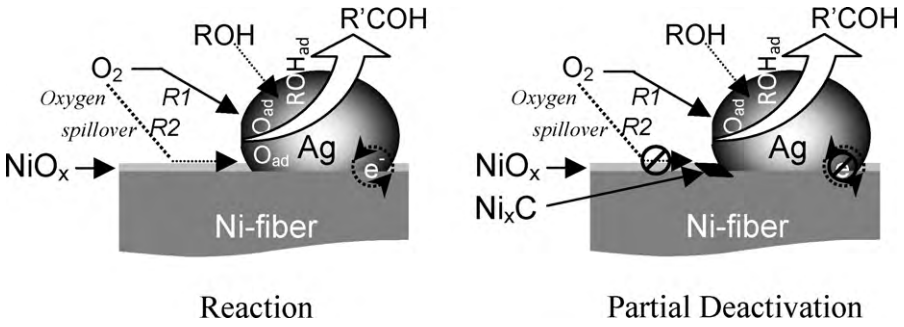

Scheme 1. Possible reaction and partial deactivation schemes for the gas-phase selective oxidation of benzyl alcohol over the Ni-microfibrous-structure supported silver catalysts. *Note:* *R*1, direct O_2 activation route; *R*2, NiO_x-participating O_2 spillover route.

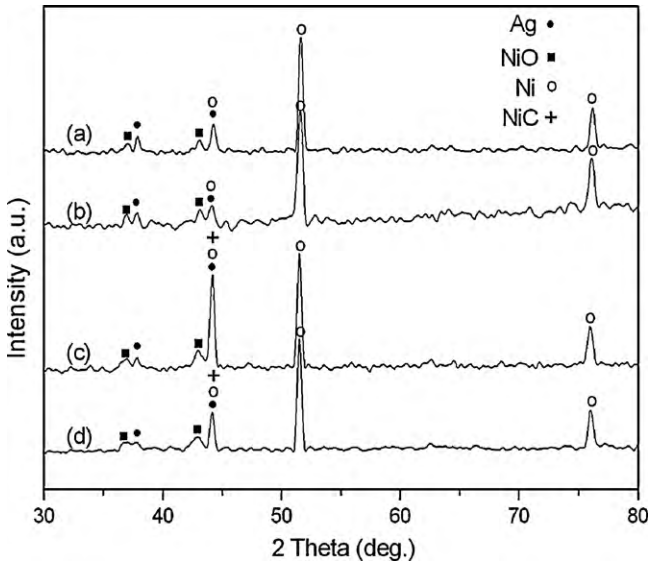

Fig. 8. XRD patterns of the Ag/Ni-fiber-M catalysts. See footnotes (a–d) in Fig. 7.

O_2-TPD experiments on the reactive, spent and regenerated samples were also carried out to study changes in the strongly chemisorbed oxygen species (denoted as O_{ad}). The amounts of O_{ad} corresponding to the O_2-desorption peak at around 650 °C were estimated and summarized in Table 1. The change is evident when comparing catalysts sampled at different reaction time points, where the O_{ad} retention fraction reduced slightly to 90% after 15 h and then drastically to 50% after 23 h (spent). This is consistent with the results shown in Fig. 6. After regeneration, the amount of O_{ad} was restored to the initial fresh catalyst level and resulted in the complete recovery of catalytic activity/selectivity.

The XRD patterns of the fresh, reactive, spent and regenerated samples are shown in Fig. 8. The reactive, spent and regenerated Ag/Ni-fiber-M samples all provide weaker Ag(1 1 1) peaks compared to the fresh catalyst. Note that this comparison was conducted at equivalent intensity of the metallic nickel XRD peak at (2θ) 51.8°. This observation agrees well with the tendency of intensity of UV band at 310–320 nm in Fig. 7, further confirming that silver tends to disperse rather than aggregate in the reaction. As also shown in Fig. 8, the XRD peak at (2θ) 44.2° is quite different from that of the Ag(1 1 1) peak. In comparison with the fresh sample, the peak intensity is increased just slightly for the sample after 15 h reaction, but considerably for the spent sample. After regeneration, the intensity of this peak is reduced significantly. Although silver and nickel metal phases can produce this peak, their contributions to the peak increase during reaction can be excluded because silver aggregation did not take place and nickel was in its bulk state. Undoubtedly, a new phase was formed in the spent catalyst sample and is assignable to Ni_xC compounds.

3.4.3. Insight into catalyst deactivation

It is known that the use of some additives (such as Co or Mn) or reactive supports can improve the activity of silver catalysts by oxygen spillover from additives or reactive supports onto the silver component [34,39,40]. In this regard and in addition to the beneficial morphology and high dispersion, nickel fiber and the small amount of NiO_x compounds in Ag/Ni-fiber-M catalyst might also serve as the reactive support and additives to promote oxygen spillover and further improve low-temperature catalytic activity.

It can be seen from Table 1 and Fig. 8 that the formation of Ni_xC phase is in good agreement with the reduction of O_{ad} amount. Clearly, the transformation of NiO_x to Ni_xC phase undoubtedly led to the interruption of the oxygen transport route where the NiO_x participated by promoting oxygen spillover. As a result, the conversion would decrease due to the reduction of O_{ad} on the silver particles.

It should be noted that the catalyst sampled at 23 h still had a high amount of O_{ad} (Table 1), being in agreement with ~75% activity maintenance after partially deactivated (Fig. 6). This suggested therefore that the direct activation of gaseous O_2 with silver particles is a main route and the NiO_2-participating oxygen-spillover route is an additive one for selective oxidation of benzyl alcohol. In accordance with the above-mentioned considerations, rational reaction and partial deactivation schemes for the gas-phase selective oxidation of benzyl alcohol are proposed and illustrated in Scheme 1.

Along with the oxygen spillover, electron transport between additives (i.e., NiO_x) and silver particles might exist through Ni-metal-fiber, which was further corroborated by the following experiments. The Ni-fiber-M support was extensively oxidized in air at 700 °C and then used to produce a series of NiO-supported silver catalysts with Ag loading ranging from 10 to 50 wt%. Unlike the Ag/Ni-fiber-M, these catalysts are not active for gas-phase selective oxidation of benzyl alcohol (conversion: <30%), suggesting that the Ni-metal-fiber is indispensable for promoting the NiO_x additive effect likely through the electron-transport mechanism (Scheme 1).

4. Conclusions

A promising thin-sheet microfibrous silver based catalyst system has been demonstrated for low temperature gas-phase selective oxidation of benzyl alcohol. The voidage tunable Ni-fiber (10–99 vol%) microfibrous structure was successfully prepared using regular wet layup papermaking/sintering method. An additional pre-wetting step with water and overnight drying was performed in order to make the Ni-fiber surface easily wettable. The catalyst that resulted in the best reactivity/selectivity was obtained by loading 10 wt% silver onto Ni-fiber followed by calcina-

tion in air at 600 °C for 4 h. It was found that enhanced wettability of the Ni-fiber support was crucial for the incorporation of more Ag cations and selectively active oxygen species of the corresponding Ag/Ni-fiber-M catalyst than the Ag/Ni-fiber catalyst using untreated support. As a result, the Ag/Ni-fiber-M catalyst exhibited much better low-temperature activity/selectivity than the Ag/Ni-fiber catalyst. In addition, the microfibrous-structured silver catalyst was shown to provide significant promotion of steady-state volumetric reaction rate compared to the electrolytic silver, attributable to the large voidage and high heat/mass transfer.

Direct activation of gaseous O_2 with silver particles is a main route and the NiO_x-participating oxygen-spillover route is an additive one for the selective oxidation of benzyl alcohol. Formation of Ni_xC compounds likely cut off O_2 activation/transportation between the NiO_x additives and silver particles thereby leading to a partial deactivation. Spent catalyst could regenerate its activity through an oxidative treatment at 400 °C. Further development is in progress to improve catalyst life-time that is particularly desirable, which includes using a different support such as titanium fiber and employing novel approaches to engineer the metal-support interaction.

Acknowledgements

We would like to thank the Shanghai Rising-Star Program (10HQ1400800), and Shanghai Leading Academic Discipline Project (B409). This work was supported by the NSFC (20590366, 20973063), the National High Technology Research and Development Program of China (2007AA05Z101), the Doctoral Fund of Ministry of Education of China (20090076110006), and the Fundamental Research Funds for the Central Universities.

References

[1] T. Mallat, A. Baiker, Chem. Rev. 104 (2004) 3037–3058.
[2] J. Shen, W. Shan, Chem. Commun. (2004) 2880–2881.
[3] R.P. Unnikrishnan, S.-D. Endalkachew, J. Catal. 211 (2002) 434–444.
[4] M. Hudlicky, Oxidation in Organic Chemistry, American Chemical Society, Washington, DC, 1990.
[5] R.A. Sheldon, J.K. Kochi, Metal-catalyzed Oxidations of Organic Compounds, Academic Press, New York, 1981.
[6] G. Cainelli, G. Cardillo, Chromium Oxidants in Organic Chemistry, Springer, Berlin, 1984.
[7] F.Z. Su, Y.-M. Liu, L.-C. Wang, Y. Cao, H.-Y. He, K.-N. Fan, Angew. Chem. Int. Ed. 47 (2008) 334–337.
[8] R.A. Sheldon, I.W.C.E. Arends, G.J.T. Brink, D.A. Green, Acc. Chem. Res. 35 (2002) 774–781.
[9] J. Shen, W. Shan, Y. Zhang, J. Du, H. Xu, K. Fan, W. Shen, Y. Tang, J. Catal. 237 (2006) 94–101.
[10] R. Yamamoto, Y. Sawayama, H. Shibahara, Y. Ichihashi, S. Nishiyama, S. Tsuruya, J. Catal. 234 (2005) 308–317.
[11] Y. Sawayama, H. Shibahara, Y. Ichihashi, S. Nishiyama, S. Tsuruya, Ind. Eng. Chem. Res. 45 (2006) 8837–8845.
[12] J.P. Mao, M.M. Deng, L. Chen, Y. Liu, Y. Lu, AIChE J. 56 (2010) 1545–1556.
[13] A.N. Pestryakov, V.V. Lunin, N.E. Bogdanchikova, V.P. Petranovskii, A. Knop-Gericke, Catal. Commun. 4 (2003) 327–331.
[14] A.N. Pestryakov, N.E. Bogdanchikova, A. Knop-Gericke, Catal. Today 91–92 (2004) 49–52.
[15] O.V. Magaev, A.S. Knyazev, O.V. Vodyankina, N.V. Dorofeeva, A.N. Salanov, A.I. Boronin, Appl. Catal. A 344 (2008) 142–149.
[16] C.D. Pina, E. Falletta, M. Rossi, J. Catal. 260 (2008) 384–386.
[17] V.R. Choudhary, P.A. Chaudhari, V.S. Narkhede, Catal. Commun. (2003) 171–175.
[18] P.T. Anastas, J.C. Warner, Green Chemistry: Theory and Practice, Oxford University Press, Oxford, 1998.
[19] Y. Lu, H. Wang, Y. Liu, Q.S. Xue, L. Chen, M.-Y. He, Lab. Chip 7 (2007) 133–140.
[20] Y. Liu, H. Wang, J.F. Li, Y. Lu, Q.S. Xue, L. Chen, AIChE J. 53 (2007) 1845–1849.
[21] M.M. Wang, J.F. Li, L. Chen, Y. Lu, Int. J. Hydrogen Energy 34 (2009) 1710–1716.
[22] Y. Liu, H. Wang, J.F. Li, Y. Lu, H.H. Wu, Q.S. Xue, L. Chen, Appl. Catal. A 328 (2007) 77–82.
[23] G.I.N. Waterhouse, G.A. Bowmaker, Appl. Catal. A 265 (2004) 85–101.
[24] G.I.N. Waterhouse, G.A. Bowmaker, Appl. Surf. Sci. 214 (2003) 36–51.
[25] A.J. Nagy, G. Mestl, D. Herein, G. Weinberg, E. Kitzelmann, R. Schlogl, J. Catal. 182 (1999) 417–429.
[26] A. Nagy, G. Mestl, Appl. Catal. A 188 (1999) 337–353.
[27] I.T.H. Chang, Z. Ren, Mater. Sci. Eng. A 120 (2004) 66–71.
[28] A.N. Pestryakov, A.A. Davydov, Appl. Catal. A 120 (1994) 7–15.
[29] M.C.N. Amorim de Carvalho, F.B. Passos, M. Schmal, J. Catal. 248 (2007) 124–129.
[30] L. Zhang, C.B. Zhang, H. He, J. Catal. 261 (2009) 101–109.
[31] Y.-E. Sung, W.Y. Lee, Korean J. Chem. Eng. 6 (1989) 300–305.
[32] C. Backx, C.P.M. de Groot, Surf. Sci. 128 (1983) 81–103.
[33] R.B. Grant, R.M. Lambert, J. Catal. 92 (1985) 364–375.
[34] Z.P. Qu, M.J. Cheng, W.X. Huang, X.H. Bao, J. Catal. 229 (2005) 446–458.
[35] B.S. Bal'zhinimaev, Kinet. Catal. 40 (1999) 795–810.
[36] N.J. Barnett, L.V. Slipchenko, M.S. Gordon, J. Phys. Chem. A 113 (2009) 7474–7481.
[37] Z.L. Zhao, Y. Niu, F. Gesmundo, C.L. Wang, Oxid. Met. 54 (2000) 559–574.
[38] H. de Monestrol, L. Schmirgeld-Mignot, P.J.A. Molinas-Mata, S. Poissonnet, G. Martin, Acta Mater. 49 (2001) 1655–1660.
[39] S. Imamura, H.R. Sawada, K. Uemura, S. Ishida, J. Catal. 109 (1988) 198–205.
[40] G.G. Xia, Y.G. Yin, W.S. Willis, J.Y. Wang, S.L. Suib, J. Catal. 185 (1999) 91–105.